Mechanistic Investigations of Palladium-Catalyzed Allylic Fluorination

Matthew H. Katcher,[†] Per-Ola Norrby,[‡,§] and Abigail G. Doyle*,[†]

[†]Department of Chemistry, Princeton University, Princeton, New Jersey 08544, United States
[‡]Department of Chemistry and Molecular Biology, University of Gothenburg, Kemigården 4, #8076, SE-412 96 Göteborg, Sweden
[§]Pharmaceutical Development, Global Medicines Development, AstraZeneca, Pepparedsleden 1, SE-431 83 Mölndal, Sweden

Ⓢ *Supporting Information*

ABSTRACT: A computational and experimental approach was employed to study the mechanism of the palladium(0)-catalyzed fluorination of allylic chlorides with AgF as fluoride source. Our findings indicate that an allylpalladium fluoride is a key intermediate necessary for the generation of both the nucleophile and electrophile. Evidence was also obtained to support a homobimetallic mechanism in which C−F bond formation occurs by nucleophilic attack of a neutral allylpalladium fluoride on a cationic allylpalladium electrophile (with fluoride as counterion). The high branched selectivity and unusual ligand effects observed in the regioselective fluorination are assessed in light of this mechanism and calculated transition states. These results may have important implications for the mechanism of other transition-metal-catalyzed fluorinations.


Calculated bimetallic transition state
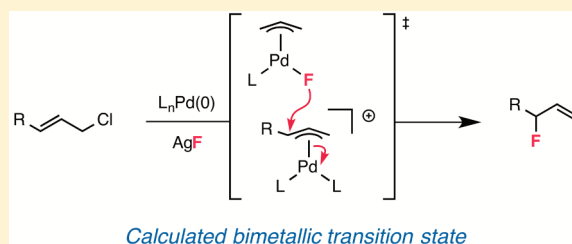
INTRODUCTION

Methods for carbon−fluorine bond formation have valuable applications in the pharmaceutical, agrochemical, radiochemical, and materials industries.[1] Although these reactions have been studied for over a century,[2] selective C−F bond formation enabled by catalysis has been the subject of intense research for only the past decade.[3] Palladium is a particularly attractive catalyst for these transformations, as it generally exhibits high functional group tolerance and a variety of ligands can be used to rationally modulate its reactivity.[4]

Initial reports of palladium-catalyzed C−F bond formation focused on the synthesis of aryl fluorides.[5] Sanford,[6] Yu,[7] and Ritter[8] have illustrated that highly oxidizing, electrophilic fluorinating reagents can allow access to high-valent Pd intermediates from which C−F reductive elimination can occur (Scheme 1a). Despite the requirement for stoichiometric Pd or directing groups in the case of catalytic reactions, the demonstration of this reactivity was a landmark achievement.[9]

An alternative strategy for Pd-catalyzed C−F bond formation relies on the reduction of an organopalladium(II) intermediate with a nucleophilic fluorine source (fluoride); this approach is especially attractive due to the lower cost and higher availability of fluoride-based reagents, in comparison to electrophilic fluorine sources.[10] For aryl fluoride synthesis, the Pd(0)/Pd(II) catalytic cycle would parallel that for traditional cross-coupling reactions,[11] with C−F bond formation occurring by inner-sphere reductive elimination from an arylpalladium fluoride intermediate (Scheme 1b). This mechanism has been well studied for other C−X reductive eliminations (X = C, N, O, S, other halides, etc.), but extensive investigations by Grushin[12] and Yandulov[13] identified distinct complications for C−F bond formation. Although C−F bond formation is thermodynami-

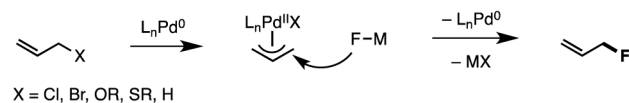## Scheme 1. Strategies for Pd-Catalyzed C−F Bond Formation
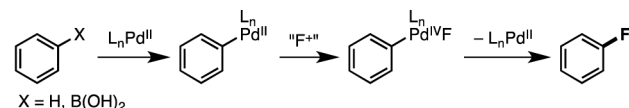
cally favored, a number of undesired side reactions (C−P, P−F, P−P bond formation) were found to be more kinetically favorable than C−F reductive elimination from an arylpalladium(II) fluoride. To overcome this challenge, Buchwald and co-workers utilized an electron-rich biarylphosphine ligand for the Pd(0)-catalyzed fluorination of aryl triflates with CsF at high temperatures.[14]

As part of a program to develop catalytic C−F bond-forming reactions with fluoride,[15] we recently identified an alternative strategy for fluorination with Pd(0)/(II) catalysis. To circumvent the aforementioned challenges associated with inner-

sphere C−F reductive elimination from Pd(II), we envisioned an outer-sphere pathway for C−F bond formation proceeding by nucleophilic attack of fluoride on an organic ligand coordinated to Pd (Scheme 1c). This mechanism could potentially operate under conditions milder than those utilized for Pd-catalyzed aryl C−F bond formation. Moreover, such an approach would complement existing technologies for aryl fluorination by providing entry into aliphatic fluorinated motifs. Initially, we targeted the reaction of fluoride with an allylpalladium intermediate to synthesize allylic fluorides, since this motif is valuable in bioactive compounds and as a synthetic intermediate.[16] Our proposed mechanism had been demonstrated for a number of other nucleophiles in Pd-catalyzed allylic substitution.[17] Furthermore, a theoretical study had indicated that outer-sphere fluoride attack on an allylpalladium intermediate is kinetically feasible.[18] However, this transformation had not been validated experimentally prior to our work.

Notably, Togni and co-workers had extensively investigated the viability of this approach to allylic fluoride synthesis.[19] Using several different fluoride sources, the authors observed no evidence for C−F bond formation in reactions with stoichiometric allylpalladium complexes ligated by bidentate P,N ligands. Instead, fluoride acted as a base to provide diene, via elimination, as the major organic product in these studies.[20] The authors also encountered an additional challenge in that the desired allylic fluoride product was shown to be unstable to their reaction conditions. In related work, Hazari, Gouverneur, and Brown have also described the Pd(0)-catalyzed alkylation of allylic fluorides with sodium malonate.[21]

As a result of these studies, we recognized that distinct conditions would be required to support a Pd-catalyzed allylic fluorination. In initial investigations toward developing a catalytic reaction, we therefore examined an extensive array of substrates and metal fluoride salts. From this evaluation, the unique combination of an allylic chloride as substrate and AgF as fluoride source provided high chemoselectivity for C−F bond formation. Application of Trost bisphosphine ligands **L1** and **L2** also afforded high enantioselectivity in the fluorination of cyclic substrates (Scheme 2a,c).[22] In further studies, we have demonstrated that these conditions are suitable for the highly regioselective synthesis of branched acyclic allylic fluorides
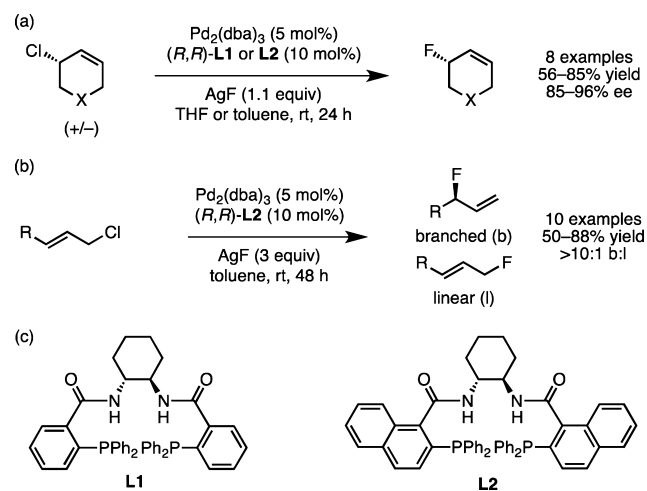
(Scheme 2b).[23] Recently, we have also extended this reactivity to the carbofluorination of allenes via a cascade reaction that also proceeds through an allylpalladium intermediate.[24]

After our initial publication, several other laboratories reported transition-metal-catalyzed allylic fluorinations that each rely on distinct combinations of catalyst, substrate, and fluoride source. Using TBAF·(t-BuOH)$_4$, Gouverneur, Brown, and co-workers have described the fluorination of allylic benzoates and carbonates under palladium and iridium catalysis.[25] Ir(I) catalysis has also been applied to the fluorination of allylic trichloroacetimidates with Et$_3$N·3HF by Nguyen and co-workers.[26] Additionally, Lauer and Wu have discovered that AgF also serves as a fluoride source for the Pd(0)-catalyzed fluorination of allylic phosphorothiorate esters.[27] Recently, several allylic fluorinations catalyzed by Rh, Cu, and Pd have also been reported with Et$_3$N·3HF as fluoride source.[28]

Despite the successful development of the aforementioned reactions for Pd(0)-catalyzed C−F bond formation, little progress has been reported toward understanding the mechanisms responsible for this reactivity.[29] Herein, we present detailed studies of Pd-catalyzed allylic fluorination with AgF aimed at understanding the mechanism of C−F bond formation from Pd(II). This work includes computational and experimental investigations that implicate an allylpalladium fluoride as a key intermediate in the Pd-catalyzed fluorination of allylic chlorides. Although C−F bond formation occurs by an outer-sphere mechanism, the proposed nucleophile and electrophile are both derived from this palladium fluoride. Furthermore, we suggest that this intermediate is responsible for the remarkable reactivity and selectivity that is observed under our optimized reaction conditions. As in other recent reports,[30] our work highlights the complex roles that transition-metal fluorides play in catalytic fluorinations.

■ RESULTS AND DISCUSSION

Initial Mechanistic Investigations. In our initial report on Pd-catalyzed allylic fluorination, the reaction mechanism was intriguing due to several conflicting observations.[22] As in our original proposal, we found that C−F bond formation occurs via an outer-sphere pathway wherein fluoride attacks the allyl ligand with inversion of stereochemistry (Scheme 3). Although

Scheme 2. Palladium-Catalyzed Allylic Fluorination of Allylic Chlorides

Scheme 3. Inversion of Stereochemistry in Outer-Sphere Fluoride Attack on an Allylpalladium Intermediate


fluoride is generally classified as a hard nucleophile due to its high charge density, this stereochemical outcome differs from that obtained in allylic substitutions with hard nucleophiles such as organomagnesium reagents and hydride. These reactions are known to proceed by retention of stereochemistry via an inner-sphere mechanism in which transmetalation of the nucleophile precedes reductive elimination.[17,31]

We also documented an important difference in the substrate requirements for allylic fluorinations and substitutions with

other nucleophiles. Although typical substrates for Pd-catalyzed asymmetric allylic alkylations include allylic acetates and carbonates, little to no C−F bond formation was observed with these substrates under the conditions we identified for allylic fluorination. Instead, allylic chlorides and bromides, which are less common substrates for Pd-catalyzed allylic substitution,[32,33] were necessary for Pd-catalyzed allylic fluorination with AgF. We initially proposed that the precipitation of AgCl provides a driving force for C−F bond formation but did not fully understand the role of this process in the overall catalytic cycle.

In the regioselective fluorination of allylic halides, we also noted several features unlike other Pd-catalyzed allylic substitutions.[23] In contrast to reactions with other nucleophiles,[34] high regioselectivity for branched allylic fluorides was obtained (Scheme 4). Although heteroatom nucleophiles

Scheme 4. Palladium-Catalyzed Regioselective Allylic Fluorination
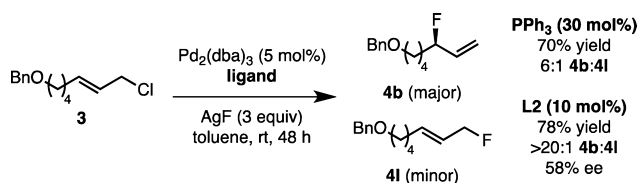
typically provide moderate selectivity for the branched product, the selectivities observed in allylic fluorination surpass those reported for reactions of amines and phenols with similar unbiased substrates (2:1 to 5:1).[35] Additionally, allylic substitutions with other nucleophiles are typically compatible with a large array of bisphosphine ligands, including dppe, dppf, and BINAP. However, good reactivity in regioselective allylic fluorination was only observed with monodentate phosphines such as PPh₃ and bidentate phosphines with large bite angles (Xantphos and **L2**).

We made the most intriguing observation relating to the mechanism of allylic C−F bond formation in the context of our stoichiometric studies on the carbofluorination of allenes.[24] In this work, we demonstrated a Heck-fluorination cascade with an aryl iodide, allene, and AgF. Mechanistically, outer-sphere C−F bond formation occurs from an allylpalladium intermediate, and stoichiometric studies indicated that a neutral allylpalladium fluoride was generated after allene insertion into the Pd−Ar bond (Scheme 5). Notably, the stoichiometric reaction of **5** and **6** proceeds with or without AgF to afford **7** in similar regioselectivity and yield. We therefore proposed that, in the Ag-free reaction, the active fluorinating reagent could be a palladium fluoride (**5**[36] or the allylpalladium fluoride

Scheme 5. Stoichiometric Carbofluorination of Allenes Proceeding via an Allylpalladium Fluoride Intermediate[a]
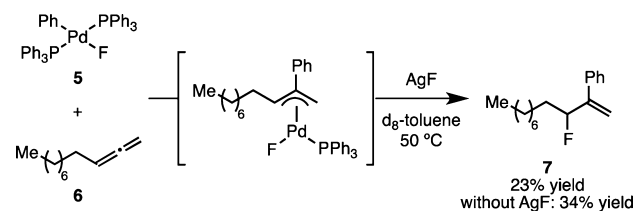
[a] >20:1 b:l for both reactions.

intermediate) or "naked" fluoride anion generated from one of these complexes.

Unfortunately, efforts to further study the mechanism of Pd-catalyzed allylic C−F bond formation in these reactions by traditional spectroscopic methods and kinetic techniques were hampered by the heterogeneity of the reaction mixtures. Although reproducible yields and selectivities could be attained with a high stir rate, reaction rates varied from run to run. We were also unable to obtain high chemo-, regio-, and enantioselectivity for fluorinations in solvents more polar than toluene and with fluoride sources more soluble than AgF.

In this work, we therefore begin by evaluating plausible reactive intermediates using theoretical methods. To support the conclusions from these studies, experiments are then performed with complexes that model potential intermediates. As a simplification, we focus on the regioselective reaction with PPh₃ as ligand. Although this reaction is not as highly regioselective as that with **L2**, it provides a more tractable experimental and computational system.[37]

Computational Methods and Potential Intermediates. DFT calculations were performed with Gaussian09,[38] and the methods were validated by comparing the solid-state structure of **8** with the calculated geometry (full details are contained in the Supporting Information). Notably, all geometry optimizations and single-point energy calculations were performed in toluene with the PCM solvent model.[39] Previous work has demonstrated that geometry optimizations in solvent are necessary to obtain transition states for the attack of fluoride on an allylpalladium intermediate.[18]

To benchmark our calculations, allylpalladium complexes **8** and **9** were synthesized,[40] and their reactivity with AgF was examined (Scheme 6). In line with analogous catalytic

**Scheme 6. Reactivity of Allylpalladium Chloride Complexes with AgF**[a]
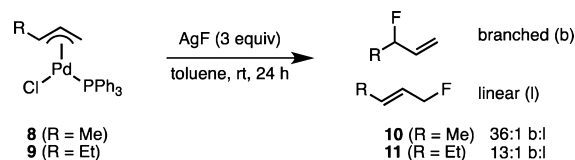
[a] Regioselectivities were determined by GC (average of three experiments). Reactions were conducted in the presence of dimethyl fumarate (1 equiv).

reactions,[41] both complexes afforded allylic fluorides with regioselectivity in favor of the branched isomer. The differences in experimental barriers leading to linear and branched products can be determined from these regioselectivities (reactions with complex **8**, $\Delta\Delta G^{\ddagger} = 9 \pm 0.7$ kJ/mol; reactions with complex **9**, $\Delta\Delta G^{\ddagger} = 6 \pm 0.5$ kJ/mol).

Potential structures for the electrophile in the allylic fluorination are shown in Chart 1. Neutral complex **A** would be the immediate product of oxidative addition, since allylic chlorides are known to react with Pd(0) to afford neutral

**Chart 1. Structures of Potential Electrophiles**
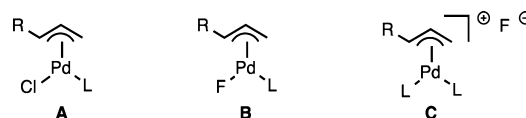
intermediates with coordinated chloride: e.g., **1**.[32c] Halide exchange between **A** and AgF would result in another potential electrophile: neutral allylpalladium fluoride **B**. Cationic complex **C** is also a possible electrophile; similar cationic complexes have been proposed in other Pd-catalyzed allylic substitutions (vide infra).[42]

We also evaluated three possible nucleophiles for Pd-catalyzed allylic fluorination. In toluene, monomeric AgF would likely bind to at least one additional ligand for stability and solubility.[43] Therefore, we investigated (PPh₃)AgF as one potential nucleophile. Phosphine−Ag complexes are well precedented:[44] for example, Yamamoto has reported asymmetric Sakurai allylations catalyzed by BINAP−AgF complexes.[45] In our reaction, only limited dissociation of PPh₃ from Pd would be necessary to ligate a catalytic amount of AgF.[46] Inspired by our studies on carbofluorination, complex **B** and "naked" fluoride in complex **C** were also included in the computational study as possible nucleophiles.

Computational Investigations of Electrophile Structure. We began our computational investigations by modeling the attack of (PPh₃)AgF (**17**) as nucleophile on neutral (**12**, **13**) and cationic (**15**, **16**) allylpalladium complexes with PPh₃ as ligand(s) (Chart 2). All complexes were assumed to undergo

Chart 2. Relevant Intermediates for Computational Studies

R = Me: **12**   R = Me: **15**   **17**
R = Et: **13**   R = Et: **16**
R = H: **14**
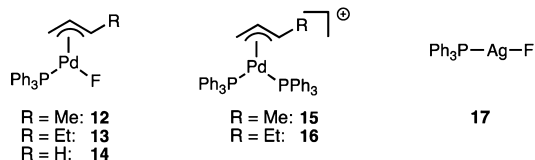
rapid apparent rotation.[47] In reactions with neutral complexes **12** and **13**, we assumed that, due to the relative trans influences of the anionic and phosphine ligands,[11a] the nucleophile would preferentially attack the allylpalladium terminus trans to the phosphine ligand (Figure S3, Supporting Information).[46,48]

For each electrophile, transition states leading to the linear and branched products were located. The energy differences between these transition states ($\Delta\Delta G^{\ddagger}$) were compared to those calculated from the experimental regioselectivities. In a smaller model system, structures approximating transition states for both syn and anti allyl isomers were located by identifying the highest point on a relaxed coordinate scan of the C−F bond. In these calculations, the estimated activation barriers for anti complexes were uniformly higher than those calculated for syn complexes (Figure S4, Supporting Information).[48] Therefore, only syn complexes were considered for the full system examined in this work.

With neutral complex **12** as the electrophile, the reaction pathways for internal and terminal attack of nucleophile **17** were computed, and the energy diagram is shown in Figure 1. Although the relative activation barriers favor production of the branched allylic fluoride, the calculated $\Delta\Delta G^{\ddagger}$ value (24 kJ/mol) is much higher than the experimental value for reactions with **8** (9 kJ/mol). For closely related transition states, using a dispersion-aware functional, we would expect the error in relative energies to be within a few kJ/mol. The discrepancy between these experimental and calculated values is outside the expected margin of error; therefore, this reaction pathway overestimates the regioselectivity.

We next considered the reaction of nucleophile **17** with cationic electrophile **15**. The full energy diagram is shown in

Figure 2, and the calculated $\Delta\Delta G^{\ddagger}$ value for these pathways (14 kJ/mol) is closer to the experimental value for reactions with complex **8** (9 kJ/mol) in comparison to that for Figure 1. With the computational methods applied here, this error is probably not significant. Although the activation barriers for these reactions are much lower than those in Figure 1, we limit our comparisons to $\Delta\Delta G^{\ddagger}$ values. Previously, it has proven difficult to compare calculated energies of charged and neutral intermediates.[49]

We also computed pathways for the reaction of nucleophile **17** and cationic complex **16**, and the calculated $\Delta\Delta G^{\ddagger}$ value is 11 kJ/mol (Figure S6, Supporting Information).[48] This value is within error of the experimental selectivity for the reaction of AgF with complex **9** (6 kJ/mol). Furthermore, the calculations reproduce the trend of lower regioselectivity with additional substitution on the allyl terminus.[50] Therefore, for two different substrates, the computational data support cationic intermediate **C**, over neutral complex **B**, as the active electrophile.

Computational Studies of Additional Nucleophiles. The data from the previous section are in reasonable agreement with silver fluoride **17** as a potential nucleophile. Since a palladium fluoride (**B**) could also serve as a nucleophile, we computed reaction pathways for neutral allylpalladium fluoride **14** as the active nucleophile. To simplify calculations, the palladium fluoride is modeled with an unsubstituted allyl ligand.

Using the methods described previously, we located transition states for the reaction of palladium fluoride **14** as nucleophile with cationic complexes **15** and **16**. The energy diagram for reaction pathways with electrophile **15** is shown in Figure 3, and the analogous diagram for reactions with electrophile **16** is presented in the Supporting Information (Figure S7). The calculated $\Delta\Delta G^{\ddagger}$ values for **14** as nucleophile are in excellent agreement with those obtained experimentally. For **15**, the calculated $\Delta\Delta G^{\ddagger}$ value is 8 kJ/mol (the experimental value is 9 kJ/mol); for **16**, calculated and experimental $\Delta\Delta G^{\ddagger}$ values are both 6 kJ/mol.

We also studied the analogous reaction between palladium fluoride **14** as nucleophile and neutral palladium fluoride **12** as electrophile, but a transition state for the linear pathway could not be located. However, the activation barrier for internal attack was calculated as 127 kJ/mol (Figure S8, Supporting Information),[48] or 25 kJ/mol higher than the analogous pathway with silver fluoride **17** as nucleophile (Figure 1). Therefore, the bimetallic reaction with **B** as nucleophile and electrophile is unlikely to compete with the other pathways considered thus far.

Finally, we attempted to model nucleophilic attack by "naked" fluoride as the counterion to cationic complex **C**. Internal ion return has been proposed for cationic intermediates with acetate and carbonate counterions,[51] and a similar process could occur from a tight ion pair with fluoride as counterion.[52] Our calculations on this mechanism were inconclusive, since the solvent model did not provide verifiable transition states. Furthermore, noncovalent interactions between fluoride and nearby C−H bonds likely distort the calculated energies. Although we cannot conclusively eliminate the participation of unligated fluoride as nucleophile, the observed chemoselectivity for C−F bond formation disfavors this mechanism. For example, Pd-catalyzed allylic fluorinations of allylic chlorides produce minimal diene (via E2 elimination) and are tolerant of silyl ethers.[22,23] This chemoselectivity does not coincide with the reactivity of other sources of "naked" fluoride that are known to be more basic[53] and to readily
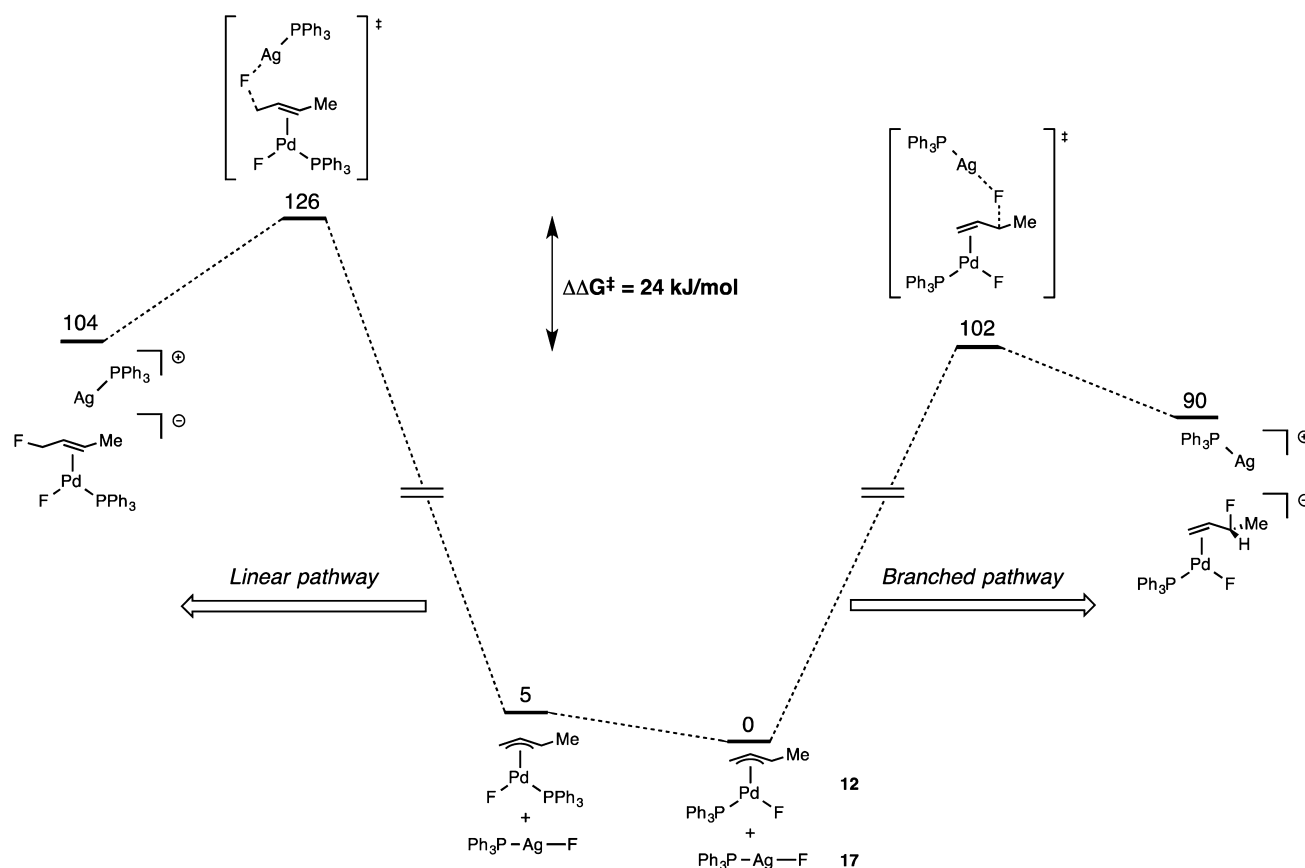
Figure 1. Energy diagram for the reaction of neutral electrophile **12** and nucleophile **17** (energies in kJ/mol).

deprotect silyl ethers.[54] Therefore, the evidence suggests that "naked" fluoride is unlikely to be the active nucleophile.

Comparing Reaction Pathways for Potential Active Nucleophiles. The regioselectivities calculated for the attack of nucleophiles **14** and **17** on cationic electrophiles **15** and **16** are both within the margin of error for the experimental values (Table 1). However, the energies for palladium fluoride **14** as nucleophile are in best agreement across the complete set of calculations. Additionally, the activation barriers for the branched pathways with **14** as nucleophile are calculated to be consistently lower (by 2−5 kJ/mol) than those with silver fluoride **17**. Although we cannot definitively exclude **17** as nucleophile, we propose that **B** is more likely to be the active nucleophile in the catalytic reactions (Table 1, entries 4 and 7). Therefore, the computational data support a homobimetallic mechanism in which neutral allylpalladium fluoride **B** acts as a nucleophile and cationic allylpalladium complex **C** acts as an electrophile.

Experimental Investigations of Electrophile Structure. Our calculations suggest that a cationic complex, with fluoride as counterion, is the electrophile in palladium-catalyzed allylic fluorination. Similarly, most Pd-catalyzed allylic substitutions with outer-sphere nucleophiles proceed via cationic intermediates with dissociated counterions such as acetate.[17,55] Conductivity studies have shown that, even in a polar solvent such as DMF, ionization of an allylpalladium chloride to a cationic complex is minimal.[42,56] However, cationic allylpalladium complexes with fluoride as counterion (**C**) have been proposed in several Pd-catalyzed allylic substitutions. Using NMR spectroscopy, Togni and co-workers have characterized a cationic allylpalladium complex resulting from the treatment of

a dimeric allylpalladium chloride complex with a bidentate ligand and TlF.[57] Hazari, Gouverneur, and Brown have also observed a cationic allylpalladium intermediate by ES-MS upon treatment of an allylic fluoride with Pd(0) and PPh₃.[21]

Nevertheless, these cationic complexes have only been shown to be competent intermediates for allylic substitutions with amines and malonates. We were also unable to observe cationic complex **C** by NMR spectroscopy in catalytic or stoichiometric fluorinations. To experimentally support the intermediacy of a cationic electrophile in allylic fluorination, we have found that allylic trifluoroacetates also undergo Pd-catalyzed allylic fluorination with AgF (Table S1, Supporting Information).[58,48] Like allylic chlorides, allylic trifluoroacetates are known to react with Pd(0) quantitatively and irreversibly, but reactions with allylic trifluoroacetates afford cationic allylpalladium complexes.[59,60]

To provide experimental evidence against a neutral electrophile such as **A** or **B**, we prepared crotylpalladium complex **20**, with a chelating *o*-diphenylphosphinobenzoate ligand, as a model for **A** and **B** that cannot readily generate **C** (Scheme 7). The geometry of **20**, with the substituted allyl terminus trans to phosphorus, was assigned in solution by examination of ¹H−³¹P NMR coupling constants.[40] The structure was also confirmed in the solid state by X-ray crystallography. Figure 4 presents an overlay of the structures of **8** and **20**, and Table 2 presents selected metrical parameters and spectroscopic data. The metrical parameters indicate that these complexes are structurally similar; despite different anionic ligands, the C−C and C−Pd bond lengths of the crotylpalladium fragment vary by less than 2% (entries 1−4). The distinct conformations of
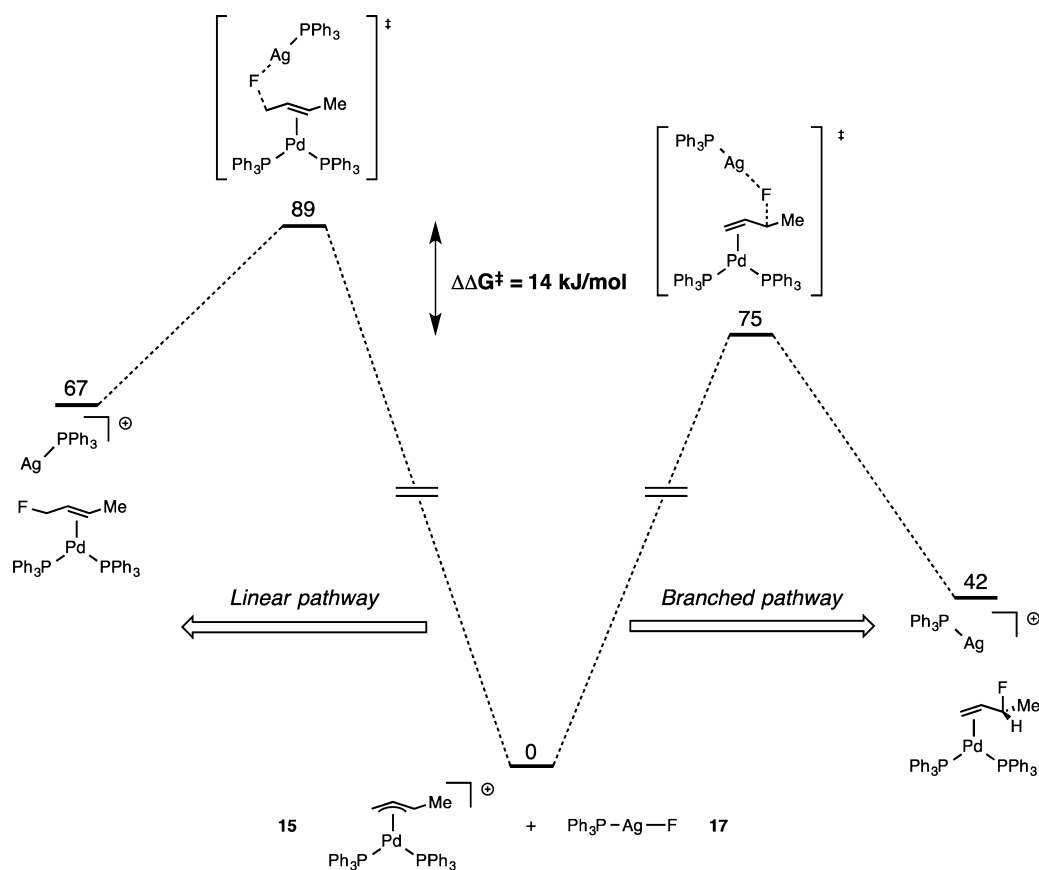
Figure 2. Energy diagram for the reaction of cationic electrophile **15** and nucleophile **17** (energies in kJ/mol).
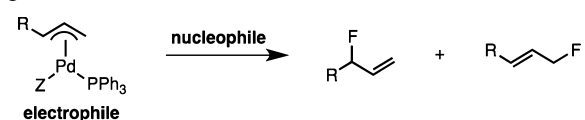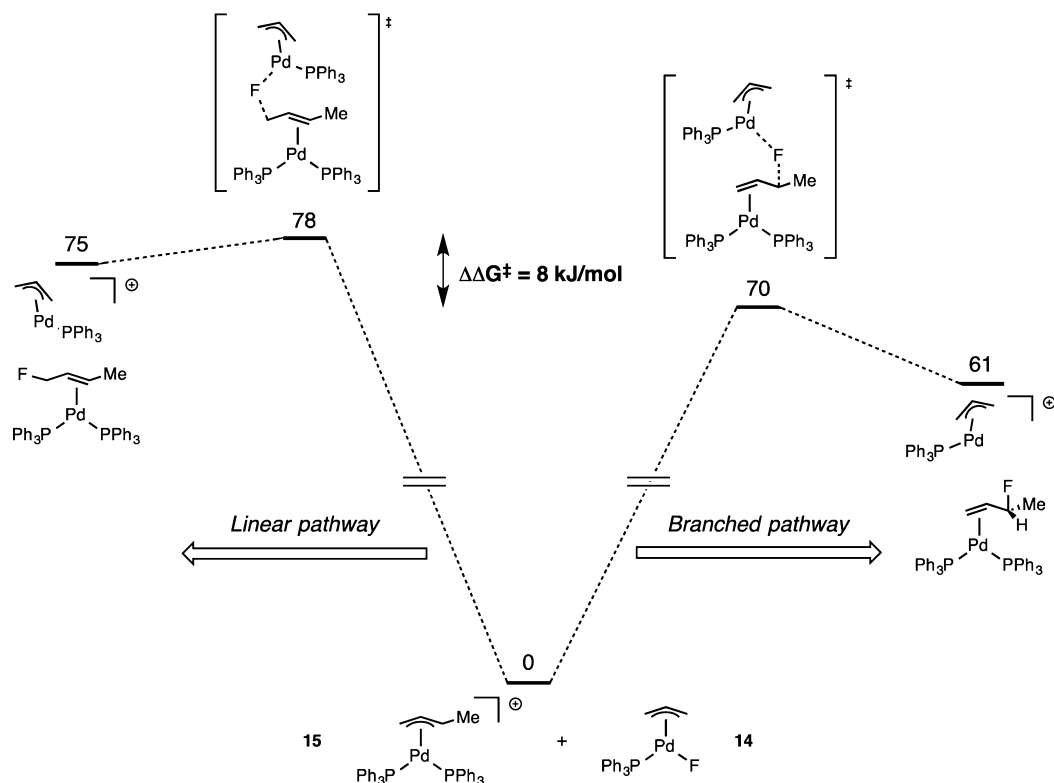

Figure 3. Energy diagram for reaction of cationic electrophile **15** and neutral palladium fluoride **14** as nucleophile (energies in kJ/mol).

the phosphine substituents in each complex do not greatly affect the bonding of and to the crotyl ligand.

Furthermore, ^{13}C NMR chemical shifts suggest that these complexes possess similar electronic characteristics. In partic-

Table 1. Summary of Experimental and Theoretical Regioselectivities

entry	R	Z	electrophile	nucleophile	$\Delta\Delta G^{\ddagger}$ (kJ/mol)
1	Me	Cl	experimental reaction: **8** + AgF		9^a
2	Me	F	**12**	**17**	24
3	Me	PPh₃	**15**	**17**	14
4	Me	PPh₃	**15**	**14**	8
5	Et	Cl	experimental reaction: **9** + AgF		6^a
6	Et	PPh₃	**16**	**17**	11
7	Et	PPh₃	**16**	**14**	6

[a]Determined from the regioselectivity of reactions in Scheme 6.

Scheme 7. Preparation of Crotylpalladium Complex 20
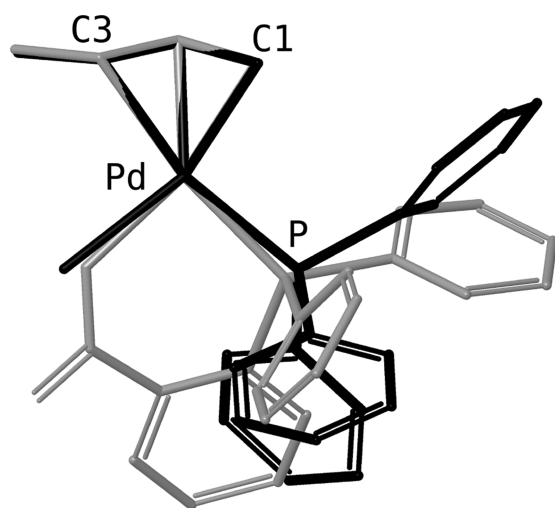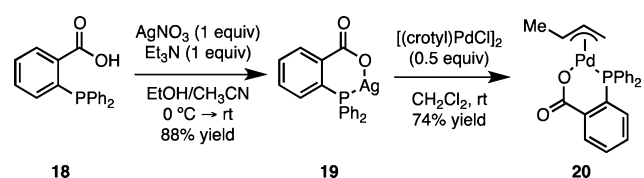
Figure 4. Overlay of solid-state structures of **8** (black) and **20** (gray) (H atoms omitted for clarity).

## Table 2. Selected Metrical Parameters and Spectroscopic Data for 8 and 20

entry	parameter	8	20
1	C1–C2 bond[a]	1.426	1.400
2	C2–C3 bond[a]	1.389	1.388
3	Pd–C1 bond[a]	2.117	2.115
4	Pd–C3 bond[a]	2.237	2.277
5	δ (¹³C NMR) C1[b]	56.59	46.04
6	δ (¹³C NMR) C3[b]	100.13	100.37

[a]Bond lengths in Å. [b]Chemical shifts in ppm.

ular, the values for C3 differ by less than 1 ppm (Table 2, entry 6). Although there is an 11 ppm difference between the chemical shifts for C1 in these complexes (entry 5),[34a,40] this disparity should not greatly affect the electrophilicity of C3,

where fluoride attack primarily occurs. Isolated allylpalladium complexes with this phosphinobenzoate ligand have not been previously described,[61] but a catalyst generated from **18** and Pd(OAc)₂ has been utilized for allylic alkylation.[62] In stoichiometric studies, allylruthenium complexes possessing this ligand react with amines and malonates,[63] and reactions of untethered allylpalladium carboxylate complexes with both inner- and outer-sphere nucleophiles are known.[64] On the basis of this precedent, we expect that complex **20** should serve as a reasonable model for a neutral allylpalladium complex in which the anionic ligand does not readily dissociate.

In the reaction between **20** and AgF, no C–F bond formation was observed (Scheme 8). The lack of productive

Scheme 8. Attempted Allylic Fluorination of 20 with AgF[a]
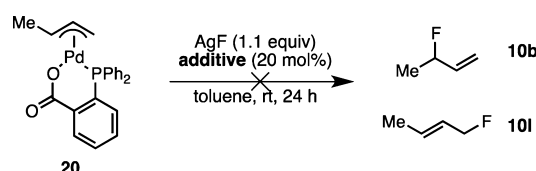
[a]additive = none, **18**, **19**. Reactions were conducted in the presence of dimethyl fumarate (1 equiv) and were analyzed by GC and ¹⁹F NMR.

reactivity with **20** may result from the absence of a ligand such as PPh₃ (in **8**) that can dissociate and enhance the solubility of AgF. To replicate this effect, the reaction of **20** and AgF was also conducted in the presence of phosphines **18** and **19** as catalytic additives, but allylic fluorides **10b** and **10l** were not produced. C–F bond formation was observed in the presence of catalytic PPh₃, but ³¹P NMR control experiments demonstrated that the mixture of PPh₃ and **20** produces an additional complex with no free PPh₃ present.[48] Therefore, the reaction with exogenous PPh₃ likely occurs via an intermediate other than **20**, and our experimental data are in agreement with the computational studies indicating that the active electrophile in Pd-catalyzed allylic fluorination is not a neutral intermediate.

Experimental Investigations of Nucleophile Structure. To further corroborate the conclusions from our calculations, we sought experimental evidence for the intermediacy and viability of a palladium fluoride as a nucleophilic species. As previously mentioned, experimental difficulties precluded kinetic studies of this proposal.[65] Furthermore, stoichiometric reactions of AgF and allylpalladium chloride **8** (or an analogous cationic complex with trifluoroacetate as counterion) were confounded by ligand equilibria between Pd and Ag species.

Fortunately, Grushin has demonstrated in related work that palladium fluoride **5** can participate in C–F bond-forming reactions with dichloromethane.[36c] Similar Pd(II) and Ni(II) fluorides are also known to fluorinate alkyl iodides and allyl bromides.[66] We found that fluorination of allylic chloride **21** with palladium fluoride **5** as fluoride source affords **22** with regioselectivity identical with that in reactions with AgF (Figure 5a). Additionally, **5** does not react with **21** in the absence of a Pd(0) catalyst, indicating that this reaction proceeds through an allylpalladium intermediate. As in the reaction with AgF, **5** also reacts with allylpalladium chloride *cis*-**1** to provide *trans*-**2** with inversion of configuration (Figure 5b, compare to Scheme 3).

These studies indicate that a palladium fluoride is a competent fluoride source for allylic fluorination and that it reacts with selectivity analogous to that with AgF. However, this outcome does not shed light on the intermediacy and
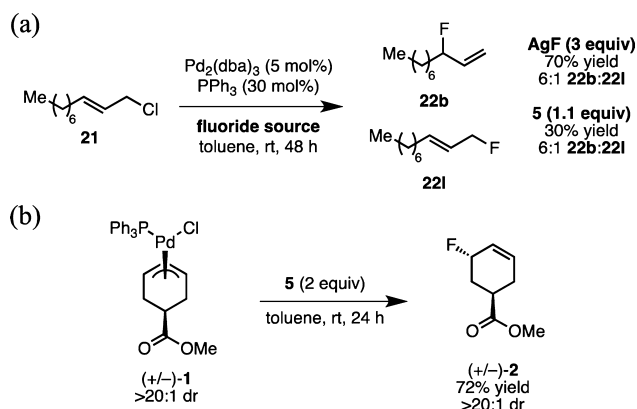
Figure 5. Allylic fluorination with **5** as fluoride source in (a) a catalytic, regioselective reaction and (b) a stoichiometric reaction with inversion of configuration (reaction conducted in the presence of dimethyl fumarate, 1 equiv).

reactivity of allylpalladium fluoride **B**. Although we were unable to observe **B** by NMR spectroscopy in these reactions, we hypothesized that **B** could be generated by halide exchange with allylpalladium chloride **A**. To model this exchange, we examined reactions of AgF and **5** with arylpalladium chloride **23** (Scheme 9). Both fluoride sources react with **23** to afford arylpalladium fluoride **24**.[67,48]

Scheme 9. Halide Exchange with Arylpalladium Chloride 23
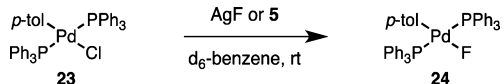
This experimental evidence suggests that allylpalladium fluoride **B** can be generated from the reaction of allylpalladium chloride **A** and AgF. Furthermore, reactions with AgF and palladium fluoride **5** both occur with identical regioselectivity. The simplest hypothesis to explain these observations is that

the active nucleophile in both reactions is a palladium fluoride. Although C−F bond formation with stoichiometric AgF as nucleophile may seem more likely than the reaction of two catalytic allylpalladium intermediates, AgF is also present in catalytic quantities as a result of its poor solubility. Along with our computational results, these experiments provide additional support for allylpalladium fluoride **B** as the active nucleophile in allylic fluorinations with AgF as fluoride source.

Support of a Homobimetallic Mechanism by Ligand Effects. Whereas we have been unable to rationalize the ligand effects observed in the regioselective allylic fluorination when considering a mechanism in which ligated AgF serves as a nucleophilic species,[68] reaction pathways with **B** as nucleophile and **C** as electrophile provide such a rationale. In this scenario, the same ligand must be capable of supporting both electrophilic and nucleophilic Pd species. Such a ligand should therefore possess intermediate electronic properties and should be capable of generating both monophosphine-ligated and diphosphine-ligated intermediates. The reactivity observed with monodentate phosphines such as PPh3 would derive from their ability to ligate the nucleophile with a single phosphine and the electrophile with two phosphines. To achieve similar coordination environments with a bidentate phosphine, ligands with large bite angles (Xantphos and **L2**) would be optimal, as one arm could dissociate to access a monoligated complex.[69] A bidentate ligand with a small bite angle, such as dppe, strongly favors cationic intermediates via the chelate effect,[70] and the necessary nucleophilic complex would be present in trace quantities.

Proposed Catalytic Cycle and Mechanism for C−F Bond Formation. Our proposed catalytic cycle for the Pd-catalyzed fluorination of allylic chlorides with PPh3 as ligand is shown in Figure 6. Coordination of the Pd(0) catalyst to the substrate, followed by oxidative addition, affords a neutral allylpalladium chloride. Halide exchange then produces a neutral allylpalladium fluoride in equilibrium with a cationic complex.[71] These two intermediates then react to forge the new
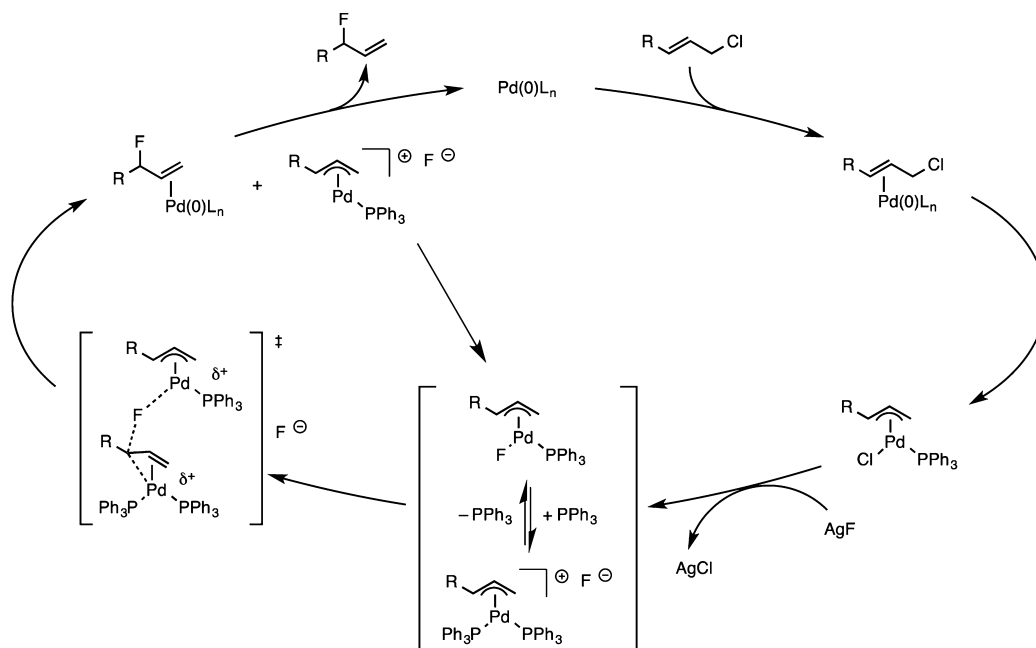

Figure 6. Proposed catalytic cycle for Pd-catalyzed allylic fluorination with C−F bond formation via a homobimetallic pathway.
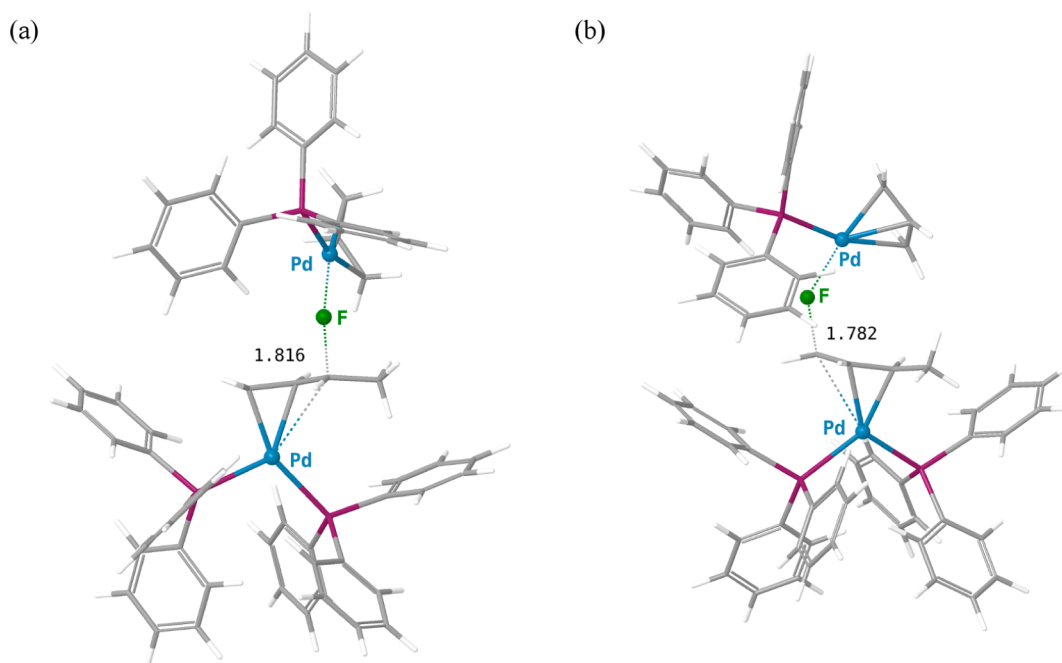
Figure 7. Transition states for internal (a) and terminal (b) attack of palladium fluoride **14** on cationic electrophile **15** (distances in Å).

C−F bond in a homobimetallic transition state. The resulting Pd(0) complex dissociates to release the allylic fluoride product and regenerate the catalyst. Additionally, the cationic Pd(II) complex remaining from the nucleophilic component re-enters the catalytic cycle in equilibrium with the neutral allylpalladium fluoride. With crotyl chloride as substrate, this transformation is exergonic by approximately 90 kJ/mol from the reactants (AgF and crotyl chloride) to the products (AgCl and the allylic fluorides).[48] The formation of AgCl and the exchange of a C−Cl bond for a C−F bond therefore provide the thermodynamic driving force for this reaction (Figure S11, Supporting Information).

Rationalization of the Regioselectivity with Calculated Transition States. Optimized transition states for reactions of cationic complexes **15** and **16** with nucleophiles **14** and **17** are late and product-like. For example, C−F bond lengths are 1.816 and 1.782 Å for internal and terminal attack, respectively, of palladium fluoride **14** on **15** (see reaction pathways in Figure 3 and structures in Figure 7).[72,48] The geometries of the transition states resemble product-like η^2-olefin complexes, with the olefin significantly rotated away from a reactant-like η^3-allyl complex.[73] By the Hammond postulate, the lateness of the transition states suggest that factors which influence the relative stability of the products should affect the relative transition state energies. In fact, the calculated $\Delta\Delta G$ values of the Pd(0)−product complexes (Figure S9, Supporting Information;[48] 8 kJ/mol for **10** and 4 kJ/mol for **11**) parallel the calculated $\Delta\Delta G^{\ddagger}$ values for reactions of **14** with **15** (8 kJ/mol) and **16** (6 kJ/mol).[74]

Notably, the transition states we located for C−F bond formation with **14** and **17** as nucleophiles are later than those that have been calculated for allylic substitutions with other nucleophiles. In transition states for the attack of stabilized carbanions on cationic allylpalladium electrophiles, forming C−C bonds are at least 2.0 Å. Furthermore, the transition states are more reactant-like than those we have identified.[37,49,75] We therefore propose that the increased regioselectivity with

fluoride, in comparison with that for other nucleophiles, results from a later transition state for C−X bond formation.

■ CONCLUSION

Our computational and experimental studies have elucidated important features in the mechanism of the Pd-catalyzed fluorination of allylic chlorides with AgF. As in Pd-catalyzed allylic substitutions with soft nucleophiles, C−F bond formation occurs by nucleophilic attack on a cationic allylpalladium intermediate. Halide exchange between an allylpalladium chloride and AgF generates both a cationic intermediate and a neutral allylpalladium fluoride. Therefore, the fluoride source must readily undergo halide exchange to generate the active nucleophile and electrophile. We propose that C−F bond formation occurs by nucleophilic attack of a neutral allylpalladium fluoride on the cationic electrophile. Since we initially anticipated challenges for C−F bond formation by inner-sphere reductive elimination, our original mechanistic proposal was devised to avoid the generation of a palladium fluoride. Unexpectedly, the mechanistic studies presented herein demonstrate that generation of a palladium fluoride is, in fact, necessary to achieve selective C−F bond formation via outer-sphere nucleophilic attack.

The proposed catalytic cycle (Figure 6) sheds some light on the questions posed at the outset of this work. In contrast with other hard nucleophiles, the reactivity of fluoride as an outer-sphere nucleophile is presumably due to its association with a transition metal. This fluorinating species is uniquely reactive, exhibiting little basicity or reactivity with traditionally fluoride-sensitive functional groups such as silyl ethers and alcohols.[22,23] Allylic acetates and carbonates fail as substrates for these fluorinations, since the allylpalladium complexes formed from these substrates do not undergo counterion exchange with a transition-metal fluoride.[76] The ligand effects observed in the regioselective reaction likely result from the requirement for a ligand that can support both electrophilic (bisphosphine) and nucleophilic (monophosphine) intermediates. Finally, in

comparison to Pd-catalyzed allylic substitutions with other nucleophiles, the high regioselectivity for fluoride attack originates from transition states that are later and more product-like than those for other nucleophiles.

Although the mechanism for C−F bond formation was studied in the context of a specific reaction, it is possible that transition-metal fluorides are key intermediates in other transition-metal-catalyzed allylic fluorinations.[25−28] Notably, Lauer and Wu's data also suggest that fluoride attacks with inversion of stereochemistry under their conditions.[27] The reactivity of palladium fluorides elucidated in our work may also have implications for other Pd(0)-catalyzed C−F bond forming reactions.

This article has focused on the factors governing reactivity and regioselectivity in Pd-catalyzed allylic fluorination, but our conclusions suggest that complex mechanisms of asymmetric induction may operate in enantioselective allylic fluorinations with **L1** and **L2**.[37] In future work, we intend to study these asymmetric reactions and apply the unique reactivity of palladium fluorides in other catalytic fluorinations.

■ EXPERIMENTAL SECTION

Computational Methods. Calculations were performed with Gaussian09,[38] with geometry optimizations using the B3LYP[77] functional and a mixed-basis set. For this set (denoted as BS1), 6-31G(d) was used on P, C, and H atoms, 6-31+G(d) was used on F and Cl atoms, and LANL2DZ with accompanying effective core potential (ECP) was used on Ag and Pd. All calculations, including geometry optimizations, were performed in toluene using the PCM solvent model.[39] Stationary points were confirmed by obtaining the correct number of imaginary frequencies. Additionally, transition states were verified to be on the reaction pathway by performing IRC calculations or by nudging the reaction coordinate along the imaginary vibrational mode, followed by energy minimization (QRC).[78] Since B3LYP is known to neglect dispersion forces,[79] we calculated single-point energies for each stationary point using the M06 functional.[80] For the single-point electronic energies, a larger mixed-basis set (BS2) was used, consisting of cc-pVTZ on P, C, and H atoms, AUG-cc-pVTZ on F and Cl atoms, and SDD with accompanying ECP on Ag and Pd. Gibbs free energies were obtained by adding these M06 electronic energies to thermal corrections obtained from frequency calculations at 298 K (B3LYP/BS1).

The computational methods were validated by comparing the calculated and experimental structures of allylpalladium chloride phosphine **8**. These structures, overlaid, with selected parameters are presented in Table S2 (Supporting Information). The calculations reproduce the geometry of **8**, with the selected bond lengths within 5%. Although the calculated structure contains Pd−ligand bond lengths that are slightly longer than those in the solid-state structure, the agreement is reasonable, considering that the structure was calculated in the solution state, while the experimental structure was obtained in the solid state.

General Experimental Methods. Unless otherwise noted, reactions were performed without the exclusion of air or moisture. Reactions using silver(I) fluoride were performed with the exclusion of light by wrapping reaction vessels in aluminum foil. Reactions were monitored by thin-layer chromatography (TLC), visualizing with fluorescence quenching, potassium permanganate (KMnO$_4$), or ceric ammonium molybdate (CAM). Organic solutions were concentrated under reduced pressure using a rotary evaporator with an ice−water bath for volatile compounds. Diethyl ether (Et$_2$O), dichloromethane (CH$_2$Cl$_2$), tetrahydrofuran (THF), toluene, 1,4-dioxane, and benzene were dried by passing through activated alumina columns; acetonitrile (CH$_3$CN), N,N-dimethylformamide (DMF), and pyridine were dried by passing through a column of activated molecular sieves.[81] d_8-Toluene and d_6-benzene were dried over activated 4 Å molecular sieves before use.

Synthesis and Characterization of Compounds. Compounds **1**,[22,32c] **5**,[36b] **8**,[40] **21**,[32f] and **23**[82] were prepared according to published procedures.

Chloro(triphenylphosphine)[(1,2,3-η)-2-pentenyl]palladium (9). A flame-dried flask was charged with palladium(II) trifluoroacetate (500 mg, 1.504 mmol). After the flask was purged under high vacuum and filled with nitrogen three times, acetone (11 mL) and 1-pentene (165 μL, 105 mg, 1.50 mmol) were placed in it. The reaction mixture was stirred at room temperature for 1 h before adding tetra-n-butylammonium chloride (460 mg, 1.65 mmol) in acetone (4 mL). After 15 min, the reaction mixture was filtered through Celite and concentrated under reduced pressure. The residue was purified by automated column chromatography (50 g silica gel, 0−15% ethyl acetate in hexanes) to afford bis[chloro((1,2,3)-η-1-pentene)-palladium] (226 mg, 0.536 mmol, 36% yield) as a yellow solid. A flame-dried flask was then charged with bis[chloro((1,2,3-η)-1-pentene)palladium] (100 mg, 0.237 mmol) and triphenylphosphine (124 mg, 0.474 mmol). After the flask was purged and filled with nitrogen three times, dichloromethane (5 mL) was added. The reaction mixture was stirred at room temperature for 20 min before adding hexanes (40 mL). The mixture was then stored overnight at −30 °C before concentrating under reduced pressure. The residue was recrystallized from ethyl acetate at −30 °C to afford the title compound (178 mg, 0.376 mmol, 79% yield) as yellow blocks: ^{1}H NMR (500 MHz, CDCl$_3$) δ 7.50−7.72 (m, 6H), 7.34−7.48 (m, 9H), 5.38 (ddd, J = 12.6, 12.6, 6.8 Hz, 1H), 4.53 (dtd, J = 12.6, 8.7, 3.9 Hz, 1H), 2.87 (dd, J = 6.8, 2.0 Hz, 1H), 2.60−2.67 (m, 1H), 2.28−2.47 (m, 1H), 2.11−2.24 (m, 1H), 1.18 (t, J = 7.4 Hz, 3H); ^{13}C NMR (125 MHz, CDCl$_3$) δ 134.15 (d, J = 12.9 Hz), 132.85 (d, J = 41.2 Hz), 130.47 (d, J = 2.2 Hz), 128.68 (d, J = 10.3 Hz), 114.90 (d, J = 4.5 Hz), 106.39 (d, J = 26.5 Hz), 56.79 (d, J = 2.1 Hz), 24.81 (d, J = 3.9 Hz), 13.43 (d, J = 5.8 Hz); ^{31}P NMR (121 MHz, CDCl$_3$) δ 24.11. Anal. Calcd for C$_{23}$H$_{24}$ClPPd: C, 58.37; H, 5.11. Found: C, 58.29; H, 5.13.

Silver 2-Diphenylphosphinobenzoate (19). A flask was charged with 2-diphenylphosphinobenzoic acid (**18**; 306 mg, 1.00 mmol), triethylamine (139 μL, 101 mg, 1.00 mmol), and ethanol (3 mL). Another flask was charged with silver nitrate (170 mg, 1.00 mmol), acetonitrile (0.3 mL), and ethanol (3 mL), and this flask was cooled to 0 °C. In the dark, the acid solution was added, dropwise, to the silver nitrate solution. The reaction mixture was then warmed to room temperature and stirred at room temperature in the dark for 2 h. The mixture was then filtered, and the filter cake was washed with cold ethanol and cold hexanes. The filter cake was then collected and dried under high vacuum to afford the title compound (346 mg, 0.837 mmol, 84% yield) as a white powder: ^{1}H NMR (500 MHz, CDCl$_3$) δ 8.11−8.26 (m, 1H), 7.52 (t, J = 7.6 Hz, 1H), 7.30−7.48 (m, 11H), 6.97 (t, J = 8.3 Hz, 1H); ^{13}C NMR (125 MHz, CDCl$_3$) δ 134.00 (d, J = 16.9 Hz), 133.80, 132.88 (d, J = 37.2 Hz), 131.94 (d, J = 10.5 Hz), 131.22, 130.62, 130.41, 130.01, 128.97 (d, J = 10.3 Hz); ^{31}P NMR (121 MHz, CDCl$_3$) δ 13.44 (d, J = 744.2 Hz).

[2-(Diphenylphosphino)benzoate-κ²P,O][(1,2,3-η)-2-butenyl]-palladium (20). An oven-dried flask was charged with crotylpalladium chloride dimer (118 mg, 0.3 mmol) and silver 2-diphenylphosphino-benzoate (**19**; 248 mg, 0.600 mmol). After it was purged under high vacuum and filled with nitrogen three times, dichloromethane (15 mL) was added. After it was stirred at room temperature for 30 min, the reaction mixture was filtered through a short plug of Celite. After concentration under reduced pressure, the residue was recrystallized from dichloromethane/hexanes to afford the title compound (206 mg, 0.441 mmol, 74% yield) as an off-white powder in a 10:1 mixture of trans and cis isomers (trans isomer: phosphine trans to the substituted allyl terminus): ^{1}H NMR (500 MHz, CDCl$_3$; cis isomer indicated by *) δ 8.31−8.36 (m, 1H*), 8.29 (ddd, J = 7.7, 4.5, 1.3 Hz, 1H), 7.26−7.54 (m, 12H, 12H*), 6.91 (dd, J = 10.1, 7.7 Hz, 1H*), 6.75 (ddd, J = 10.4, 7.8, 1.3 Hz, 1H), 5.52−5.60 (m, 1H*), 5.48 (ddd, J = 12.3, 12.3, 6.8 Hz, 1H), 4.68−4.77 (m, 1H*), 4.67 (ddq, J = 12.8, 9.4, 6.5 Hz, 1H), 3.78 (dd, J = 13.8, 9.5 Hz, 1H*), 3.42−3.54 (m, 1H*), 3.10 (dd, J = 6.7, 2.6 Hz, 1H), 2.60 (dm, J = 11.7 Hz, 1H), 1.78 (dd, J = 9.0, 6.3 Hz, 3H), 0.86 (dd, J = 8.6, 6.3 Hz, 3H*); ^{13}C NMR (125 MHz, CDCl$_3$; cis isomer indicated by * when identifiable) δ 171.44 (d, J =

5.1 Hz), 170.74* (d, J = 5.0 Hz), 144.33 (d, J = 16.1 Hz), 143.52* (d, J = 15.5 Hz), 133.81 (d, J = 14.0 Hz), 133.73* (d, J = 13.5 Hz), 133.40* (d, J = 8.9 Hz), 133.35 (d, J = 9.2 Hz), 132.23* (d, J = 2.1 Hz), 132.13 (d, J = 2.3 Hz), 131.08 (d, J = 2.1 Hz), 130.60 (d, J = 13.3 Hz), 129.51 (d, J = 6.7 Hz), 129.17 (d, J = 21.9 Hz), 129.17, 127.23* (d, J = 40.0 Hz), 126.69 (d, J = 40.0 Hz), 120.89* (d, J = 5.6 Hz), 117.69 (d, J = 4.6 Hz), 100.37 (d, J = 26.2 Hz), 78.48* (d, J = 28.2 Hz), 65.82* (d, J = 5.4 Hz), 46.04 (d, J = 3.7 Hz), 17.59*, 17.32 (d, J = 4.0 Hz); ^{31}P NMR (203 MHz, CDCl$_3$; cis isomer indicated by *) δ 21.84, 19.18*. Anal. Calcd for C$_{23}$H$_{21}$O$_2$PPd: C, 59.18; H, 4.53. Found: C, 58.25; H, 4.35.

General Procedure for Reactions with Stoichiometric Allylpalladium Complexes 8, 9, and 20. To oven-dried 1 dram borosilicate vials, the appropriate palladium complex (8, 9, or 20; 0.05 mmol), dimethyl fumarate (7.2 mg, 0.05 mmol), and silver(I) fluoride (19 mg, 0.15 mmol) were added (along with an additive, as appropriate). Three times, the vials were purged under high vacuum and filled with nitrogen. Then, each vial was charged with toluene (1 mL). After they were stirred at 700 rpm for 24 h (with the vials covered in aluminum foil), the reaction mixtures were filtered through short plugs of silica gel, with toluene as eluent. Regioselectivity was determined by GC using a commercial column, and the reported regioselectivities are the average of three runs. Spectral data for **10b,l** were in agreement with literature values.[83]

(±)-3-Fluoropent-1-ene (**11b**) and (E)-1-fluoropent-2-ene (**11l**): ^{1}H NMR (500 MHz, CDCl$_3$, linear isomer indicated by *) δ 5.50–5.94 (m, 1H, 2H*), 5.26–5.35 (m, 1H), 5.22 (dt, J = 10.7, 1.4 Hz, 1H), 4.65–4.92 (m, 1H, 2H*), 2.00–2.16 (m, 2H*), 1.61–1.82 (m, 2H), 1.02 (t, J = 7.5 Hz, 3H), 0.96 (t, J = 7.5 Hz, 3H); ^{13}C NMR (125 MHz, CDCl$_3$, linear isomer indicated by *) δ 139.29* (d, ^3J = 12.0 Hz), 136.44 (d, ^2J = 19.7 Hz), 123.47* (d, ^2J = 16.5 Hz), 117.04 (d, ^3J = 11.9 Hz), 94.91 (d, ^1J = 166.8 Hz), 83.87* (d, ^1J = 159.6 Hz), 28.22 (d, ^2J = 22.6 Hz), 25.25* (d, ^4J = 2.3 Hz), 13.01*, 8.96 (d, ^3J = 6.0 Hz); ^{19}F NMR (282 MHz, CDCl$_3$, linear isomer indicated by *) δ −177.87 (m), −207.24* (m).

Reactions with Palladium Fluoride 5 as Fluoride Source. A 0.05 M stock solution was prepared in toluene (1 mL/reaction), containing (E)-1-chlorodec-2-ene (**21**; 5.2 mg, 0.03 mmol/reaction, 1 equiv) and dodecane (2.7 μL/reaction, 40 mol %). An aliquot was reserved for measurement of the initial ratio by GC. To an oven-dried 1 dram borosilicate vial, tris(dibenzylideneacetone)dipalladium (1.4 mg, 0.0015 mmol), triphenylphosphine (2.4 mg, 0.009 mmol), and trans-bis(triphenylphosphine)phenylpalladium fluoride (**5**; 24 mg, 0.033 mmol) were added. Three times, the vial was purged under high vacuum and filled with nitrogen. Then, the vial was charged with the stock solution (0.6 mL). After it was stirred at 700 rpm for 48 h (with the vial covered in aluminum foil), the reaction mixture was filtered through a short plug of silica gel, with 10% ether in hexanes as eluent. Conversion, yield, and regioselectivity were determined by GC using a commercial column (a response factor was calculated using ^{1}H NMR). Spectral data for **22b,l** were in agreement with literature values.[84]

For the determination of background reaction between **21** and **5**, the same procedure was followed, omitting tris-(dibenzylideneacetone)dipalladium and PPh$_3$. No allylic fluorides were detected by GC.

To an oven-dried 1 dram borosilicate vial, chloro-(triphenylphosphine)[cis-5-carbomethoxy-(1,2,3-η)-cyclohexenyl]-palladium (**1**; 14 mg, 0.025 mmol), dimethyl fumarate (3.6 mg, 0.025 mmol), and trans-bis(triphenylphosphine)phenylpalladium fluoride (**5**; 36 mg, 0.05 mmol) were added. Three times, the vial was purged under high vacuum and filled with nitrogen. Then, the vial was charged with d_8-toluene (0.5 mL). After it was stirred at 700 rpm for 24 h (with the vial covered in aluminum foil), the reaction mixture was charged with a solution of an internal standard (1,4-difluorobenzene, 40 mol %) in d_8-toluene. The reaction mixture was then filtered through a short plug of Celite, with d_8-toluene as eluent. Diastereoselectivity (>20:1 dr) and yield (72%) were determined by ^{19}F NMR. Spectral data for **2** were in agreement with literature values.[21]

Halide Exchange with Arylpalladium Chloride. To oven-dried 1 dram borosilicate vials, trans-bis(triphenylphosphine)(p-tolyl)palladium chloride (**23**; 15 mg, 0.02 mmol) and the appropriate fluoride source (0.02 mmol) were added. Three times, the vials were purged under high vacuum and filled with nitrogen. Then, the vials were charged with d_6-benzene (1 mL). The mixtures were stirred at 700 rpm, and at various time points aliquots from the reaction mixtures were filtered through short plugs of Celite, with d_6-benzene as eluent. The reactions were then analyzed by ^{31}P NMR to observe the formation of trans-bis(triphenylphosphine)(p-tolyl)palladium fluoride (**24**).[36b]

ASSOCIATED CONTENT

$\mathbf{S}$ Supporting Information

Text, figures, tables, and CIF files giving additional experimental details, X-ray crystallographic data for **8** and **20**, additional energy diagrams, calculated structures and energies, and the full ref 38. This material is available free of charge via the Internet at http://pubs.acs.org.

AUTHOR INFORMATION

Corresponding Author
*E-mail for A.G.D.: agdoyle@princeton.edu.

Notes
The authors declare no competing financial interest.

ACKNOWLEDGMENTS

REFERENCES

(1) (a) Banks, R. E., Smart, B. E., Tatlow, J. C., Eds. *Organofluorine Chemistry: Principles and Commercial Applications*; Plenum Press: New York, 1994. (b) Müller, K.; Faeh, C.; Diederich, F. *Science* **2007**, *317*, 1881–1886. (c) Purser, S.; Moore, P. R.; Swallow, S.; Gouverneur, V. *Chem. Soc. Rev.* **2008**, *37*, 320–330. (d) Jeschke, P. *ChemBioChem* **2004**, *5*, 570–589. (e) Cai, L.; Lu, S.; Pike, V. W. *Eur. J. Org. Chem.* **2008**, 2853–2873.

(2) For the synthesis of benzoyl fluoride from benzoyl chloride and potassium bifluoride, see: Borodine, A. *Justus Liebigs Ann. Chem.* **1863**, *126*, 58–62.

(3) (a) Ma, J.-A.; Cahard, D. *Chem. Rev.* **2008**, *108*, PR1–PR43. (b) Lectard, S.; Hamashima, Y.; Sodeoka, M. *Adv. Synth. Catal.* **2010**, *352*, 2708–2732. (c) Furuya, T.; Kamlet, A. S.; Ritter, T. *Nature* **2011**, *473*, 470–477. (d) Hollingworth, C.; Gouverneur, V. *Chem. Commun.* **2012**, *48*, 2929–2942.

(4) Negishi, E.-i., Ed. *Handbook of Organopalladium Chemistry for Organic Synthesis*; Wiley: New York, 2002.

(5) For a review on aryl fluoride synthesis, see: Furuya, T.; Klein, J. E. M. N.; Ritter, T. *Synthesis* **2010**, 1804–1821.

(6) (a) Hull, K. L.; Anani, W. Q.; Sanford, M. S. *J. Am. Chem. Soc.* **2006**, *128*, 7134–7135. (b) Ball, N. D.; Sanford, M. S. *J. Am. Chem. Soc.* **2009**, *131*, 3796–3797.

(7) (a) Wang, X.; Mei, T.-S.; Yu, J.-Q. *J. Am. Chem. Soc.* **2009**, *131*, 7520−7521. (b) Chan, K. S. L.; Wasa, M.; Wang, X.; Yu, J.-Q. *Angew. Chem., Int. Ed.* **2011**, *50*, 9081−9084.

(8) (a) Furuya, T.; Kaiser, H. M.; Ritter, T. *Angew. Chem., Int. Ed.* **2008**, *47*, 5993−5996. (b) Furuya, T.; Ritter, T. *J. Am. Chem. Soc.* **2008**, *130*, 10060−10061. (c) Furuya, T.; Benitez, D.; Tkatchouk, E.; Strom, A. E.; Tang, P.; Goddard, W. A.; Ritter, T. *J. Am. Chem. Soc.* **2010**, *132*, 3793−3807. For related applications of this chemistry to ^{18}F fluorination, see: (d) Lee, E.; Kamlet, A. S.; Powers, D. C.; Neumann, C. N.; Boursalian, G. B.; Furuya, T.; Choi, D. C.; Hooker, J. M.; Ritter, T. *Science* **2011**, *334*, 639−642. (e) Kamlet, A. S.; Neumann, C. N.; Lee, E.; Carlin, S. M.; Moseley, C. K.; Stephenson, N.; Hooker, J. M.; Ritter, T. *PLoS ONE* **2013**, *8*, e59187.

(9) For examples of aliphatic C−F bond formation from high-valent Pd, see: (a) Qiu, S.; Xu, T.; Zhou, J.; Guo, Y.; Liu, G. *J. Am. Chem. Soc.* **2010**, *132*, 2856−2857. (b) Qiu, S.; Xu, T.; Zhou, J.; Guo, Y.; Liu, G. *J. Am. Chem. Soc.* **2010**, *132*, 2856−2857. (c) Racowski, J. M.; Gary, J. B.; Sanford, M. S. *Angew. Chem., Int. Ed.* **2012**, *51*, 3414−3417. (d) McMurtrey, K. B.; Racowski, J. M.; Sanford, M. S. *Org. Lett.* **2012**, *14*, 4094−4097. For a related example of Pd-catalyzed vinyl fluoride synthesis, see: (e) Peng, H.; Liu, G. *Org. Lett.* **2011**, *13*, 772−775.

(10) Furuya, T.; Kuttruff, C. A.; Ritter, T. *Curr. Opin. Drug Discovery Dev.* **2008**, *11*, 803−819.

(11) (a) Hartwig, J. *Organotransition Metal Chemistry*; University Science Books: Sausalito, CA, 2010. (b) Johansson Seechurn, C. C. C.; Kitching, M. O.; Colacot, T. J.; Snieckus, V. *Angew. Chem., Int. Ed.* **2012**, *51*, 5062−5085.

(12) (a) Grushin, V. V. *Chem. Eur. J.* **2002**, *8*, 1006−1014. (b) Grushin, V. V. *Acc. Chem. Res.* **2010**, *43*, 160−171.

(13) Yandulov, D. V.; Tran, N. T. *J. Am. Chem. Soc.* **2007**, *129*, 1342−1358.

(14) (a) Watson, D. A.; Su, M.; Teverovskiy, G.; Zhang, Y.; García-Fortanet, J.; Kinzel, T.; Buchwald, S. L. *Science* **2009**, *325*, 1661−1664. (b) Noël, T.; Maimone, T. J.; Buchwald, S. L. *Angew. Chem., Int. Ed.* **2011**, *50*, 8900−8903. (c) Wannberg, J.; Wallinder, C.; Ünlüsoy, M.; Sköld, C.; Larhed, M. *J. Org. Chem.* **2013**, *78*, 4184−4189. (d) Lee, H. G.; Milner, P. J.; Buchwald, S. L. *Org. Lett.* **2013**, *15*, 5602−5605.

(15) (a) Kalow, J. A.; Doyle, A. G. *J. Am. Chem. Soc.* **2010**, *132*, 3268−3269. (b) Kalow, J. A.; Doyle, A. G. *J. Am. Chem. Soc.* **2011**, *133*, 16001−16012. (c) Shaw, T. W.; Kalow, J. A.; Doyle, A. G. *Org. Synth.* **2012**, *89*, 9−18. (d) Kalow, J. A.; Schmitt, D. E.; Doyle, A. G. *J. Org. Chem.* **2012**, *77*, 4177−4183. (e) Kalow, J. A.; Doyle, A. G. *Tetrahedron* **2013**, *69*, 5702−5709.

(16) Pacheco, M. C.; Purser, S.; Gouverneur, V. *Chem. Rev.* **2008**, *108*, 1943−1981.

(17) (a) Trost, B. M.; Van Vranken, D. L. *Chem. Rev.* **1996**, *96*, 395−422. (b) Lu, Z.; Ma, S. *Angew. Chem., Int. Ed.* **2008**, *47*, 258−297. (c) Trost, B. M.; Zhang, T.; Sieber, J. D. *Chem. Sci.* **2010**, *1*, 427−440.

(18) Hagelin, H.; Åkermark, B.; Norrby, P.-O. *Chem. Eur. J.* **1999**, *5*, 902−909.

(19) Hintermann, L.; Läng, F.; Maire, P.; Togni, A. *Eur. J. Inorg. Chem.* **2006**, 1397−1412.

(20) Clark, J. H. *Chem. Rev.* **1980**, *80*, 429−452.

(21) Hazari, A.; Gouverneur, V.; Brown, J. M. *Angew. Chem., Int. Ed.* **2009**, *48*, 1296−1299.

(22) Katcher, M. H.; Doyle, A. G. *J. Am. Chem. Soc.* **2010**, *132*, 17402−17404.

(23) Katcher, M. H.; Sha, A.; Doyle, A. G. *J. Am. Chem. Soc.* **2011**, *133*, 15902−15905.

(24) Braun, M.-G.; Katcher, M. H.; Doyle, A. G. *Chem. Sci.* **2013**, *4*, 1216−1220.

(25) (a) Hollingworth, C.; Hazari, A.; Hopkinson, M. N.; Tredwell, M.; Benedetto, E.; Huiban, M.; Gee, A. D.; Brown, J. M.; Gouverneur, V. *Angew. Chem., Int. Ed.* **2011**, *50*, 2613−2617. (b) E. Benedetto, E.; Tredwell, M.; Hollingworth, C.; Khotavivattana, T.; Brown, J. M.; Gouverneur, V. *Chem. Sci.* **2013**, *4*, 89−96.

(26) Topczewski, J. J.; Tewson, T. J.; Nguyen, H. M. *J. Am. Chem. Soc.* **2011**, *133*, 19318−19321.

(27) Lauer, A. M.; Wu, J. *Org. Lett.* **2012**, *14*, 5138−5141.

(28) (a) Zhu, J.; Tsui, G. C.; Lautens, M. *Angew. Chem., Int. Ed.* **2012**, *51*, 12353−12356. (b) Zhang, Z.; Wang, F.; Mu, X.; Chen, P.; Liu, G. *Angew. Chem., Int. Ed.* **2013**, *52*, 7549−7553. (c) Braun, M.-G.; Doyle, A. G. *J. Am. Chem. Soc.* **2013**, *135*, 12990−12993. (d) Zhang, Q.; Nguyen, H. M. *Chem. Sci.* **2014**, *5*, 291−296.

(29) For mechanistic studies on C−F bond formation from Pd(IV) intermediates, see refs 6b, 8c, and 9c.

(30) For examples, see: (a) Reference 15b. (b) Liu, W.; Huang, X.; Cheng, M.-J.; Nielsen, R. J.; Goddard, W. A.; Groves, J. T. *Science* **2012**, *337*, 1322−1325. (c) Barthazy, P.; Togni, A.; Mezzetti, A. *Organometallics* **2001**, *20*, 3472−3477.

(31) (a) Keinan, E.; Roth, Z. *J. Org. Chem.* **1983**, *48*, 1769−1772. (b) Fiaud, J. C.; Legros, J. Y. *J. Org. Chem.* **1987**, *52*, 1907−1911.

(32) For examples, see: (a) Sheffy, F. K.; Godschalx, J. P.; Stille, J. K. *J. Am. Chem. Soc.* **1984**, *106*, 4833−4840. (b) Goliaszewski, A.; Schwartz, J. *Organometallics* **1985**, *4*, 417−419. (c) Kurosawa, H.; Kajimaru, H.; Ogoshi, S.; Yoneda, H.; Miki, K.; Kasai, N.; Murai, S.; Ikeda, I. *J. Am. Chem. Soc.* **1992**, *114*, 8417−8424. (d) Matsumoto, Y.; Ohno, A.; Hayashi, T. *Organometallics* **1993**, *12*, 4051−4055. (e) Albéniz, A. C.; Espinet, P.; Martín-Ruiz, B. *Chem. Eur. J.* **2001**, *7*, 2481−2489. (f) Brozek, L. A.; Ardolino, M. J.; Morken, J. P. *J. Am. Chem. Soc.* **2011**, *133*, 16778−16781.

(33) These substrates are more common in Cu-catalyzed allylic substitution: Falciola, C. A.; Alexakis, A. *Eur. J. Org. Chem.* **2008**, 3765−3780.

(34) (a) Åkermark, B.; Zetterberg, K.; Hansson, S.; Krakenberger, B.; Vitagliano, A. *J. Organomet. Chem.* **1987**, *335*, 133−142. (b) Trost, B. M.; Ariza, X. *J. Am. Chem. Soc.* **1999**, *121*, 10727−10737.

(35) (a) Goux, C.; Lhoste, P.; Sinou, D. *Synlett* **1992**, 725−727. (b) Trost, B. M.; Toste, F. D. *J. Am. Chem. Soc.* **1999**, *121*, 4545−4554. (c) Dubovyk, I.; Watson, I. D. G.; Yudin, A. K. *J. Org. Chem.* **2013**, *78*, 1559−1575.

(36) (a) Fraser, S. L.; Antipin, M. Y.; Khroustalyov, V. N.; Grushin, V. V. *J. Am. Chem. Soc.* **1997**, *119*, 4769−4770. (b) Pilon, M. C.; Grushin, V. V. *Organometallics* **1998**, *17*, 1774−1781. (c) Grushin, V. V. *Angew. Chem., Int. Ed.* **1998**, *37*, 994−996.

(37) Butts, C. P.; Filali, E.; Lloyd-Jones, G. C.; Norrby, P.-O.; Sale, D. A.; Schramm, Y. *J. Am. Chem. Soc.* **2009**, *131*, 9945−9957.

(38) Frisch, M. J., et al. *Gaussian 09, revision C.01*; Gaussian, Inc., Wallingford, CT, 2010.

(39) Tomasi, J.; Mennucci, B.; Cammi, R. *Chem. Rev.* **2005**, *105*, 2999−3094.

(40) Åkermark, B.; Krakenberger, B.; Hansson, S.; Vitagliano, A. *Organometallics* **1987**, *6*, 620−628.

(41) In the catalytic reaction with (E)-crotyl chloride as substrate, an 18:1 b:l ratio was obtained.

(42) (a) Åkermark, B.; Åkermark, G.; Hegedus, L. S.; Zetterberg, K. *J. Am. Chem. Soc.* **1981**, *103*, 3037−3040. (b) Cantat, T.; Génin, E.; Giroud, C.; Meyer, G.; Jutand, A. *J. Organomet. Chem.* **2003**, *687*, 365−376.

(43) ^{19}F NMR studies indicated that the solubility of AgF in toluene is in the picomolar to nanomolar range.

(44) Although we did not observe ^{31}P NMR evidence for PPh$_3$−Ag binding, the NMR signals of a related complex are broad, due to rapid ligand exchange: Létinois-Halbes, U.; Pale, P.; Berger, S. *Magn. Reson. Chem.* **2004**, *42*, 831−834.

(45) (a) Yanagisawa, A.; Kageyama, H.; Nakatsuka, Y.; Asakawa, K.; Matsumoto, Y.; Yamamoto, H. *Angew. Chem., Int. Ed.* **1999**, *38*, 3701−3703. (b) Wadamoto, M.; Yamamoto, H. *J. Am. Chem. Soc.* **2005**, *127*, 14556−14557.

(46) Svensen, N.; Fristrup, P.; Tanner, D.; Norrby, P.-O. *Adv. Synth. Catal.* **2007**, *349*, 2631−2640.

(47) Hansson, S.; Norrby, P. O.; Sjögren, M. P. T.; Åkermark, B.; Cucciolito, M. E.; Giordano, F.; Vitagliano, A. *Organometallics* **1993**, *12*, 4940−4948.

(48) See the Supporting Information for details.

(49) Fristrup, P.; Ahlquist, M.; Tanner, D.; Norrby, P.-O. *J. Phys. Chem. A* **2008**, *112*, 12862−12867.

(50) Notably, **16** has several more accessible conformations than **15** (Figure S5, Supporting Information); $\Delta\Delta G^{\ddagger}$ was calculated for the transition states with the lowest energies of all reaction pathways examined. Although a transition state was found for internal attack of silver fluoride **17** on the neutral electrophile **13**, a transition state for the analogous terminal attack could not be located.

(51) Evans, L. A.; Fey, N.; Harvey, J. N.; Hose, D.; Lloyd-Jones, G. C.; Murray, P.; Orpen, A. G.; Osborne, R.; Owen-Smith, G. J. J.; Purdie, M. *J. Am. Chem. Soc.* **2008**, *130*, 14471−14473.

(52) Ion pairs with anions as outer-sphere nucleophiles have also been invoked in the asymmetric allylic alkylation of enol carbonates: Trost, B. M.; Xu, J.; Schmidt, T. *J. Am. Chem. Soc.* **2009**, *131*, 18343−18357.

(53) (a) Christe, K. O.; Wilson, W. W.; Wilson, R. D.; Bau, R.; Feng, J. A. *J. Am. Chem. Soc.* **1990**, *112*, 7619−7625. (b) Schwesinger, R.; Link, R.; Thiele, G.; Rotter, H.; Honert, D.; Limbach, H.-H.; Männle, F. *Angew. Chem., Int. Ed. Engl.* **1991**, *30*, 1372−1375.

(54) (a) Holton, R. A.; Kim, H. B.; Somoza, C.; Liang, F.; Biediger, R. J.; Boatman, P. D.; Shindo, M.; Smith, C. C.; Kim, S. *J. Am. Chem. Soc.* **1994**, *116*, 1599−1600. (b) Wender, P. A.; Badham, N. F.; Conway, S. P.; Floreancig, P. E.; Glass, T. E.; Houze, J. B.; Krauss, N. E.; Lee, D.; Marquess, D. G.; McGrane, P. L.; Meng, W.; Natchus, M. G.; Shuker, A. J.; Sutton, J. C.; Taylor, R. E. *J. Am. Chem. Soc.* **1997**, *119*, 2757−2758. (c) Carpenter, J.; Northrup, A. B.; Chung, D. M.; Wiener, J. J. M.; Kim, S.-G.; MacMillan, D. W. C. *Angew. Chem., Int. Ed.* **2008**, *47*, 3568−3572.

(55) (a) Åkermark, B.; Hansson, S.; Krakenberger, B.; Vitagliano, A.; Zetterberg, K. *Organometallics* **1984**, *3*, 679−682. (b) Amatore, C.; Gamez, S.; Jutand, A.; Meyer, G.; Mottier, L. *Electrochim. Acta* **2001**, *46*, 3237−3244.

(56) In this work, we assume that the active electrophile is an η^3-allyl rather than an η^1-allyl palladium complex. This assumption is supported by other studies indicating that η^1-allyl palladium intermediates are usually nucleophilic. See: (a) Nakamura, H.; Bao, M.; Yamamoto, Y. *Angew. Chem., Int. Ed.* **2001**, *40*, 3208−3210. (b) Solin, N.; Kjellgren, J.; Szabó, K. J. *J. Am. Chem. Soc.* **2004**, *126*, 7026−7033. (c) García-Iglesias, M.; Buñuel, E.; Cárdenas, D. J. *Organometallics* **2006**, *25*, 3611−3618.

(57) Burckhardt, U.; Baumann, M.; Togni, A. *Tetrahedron: Asymmetry* **1997**, *8*, 155−159.

(58) For examples of Pd(0)-catalyzed allylic substitutions of allylic trifluoroacetates, see: (a) Obora, Y.; Ogawa, Y.; Imai, Y.; Kawamura, T.; Tsuji, Y. *J. Am. Chem. Soc.* **2001**, *123*, 10489−10493. (b) Obora, Y.; Nakanishi, M.; Tokunaga, M.; Tsuji, Y. *J. Org. Chem.* **2002**, *67*, 5835−5837. (c) Grote, R. E.; Jarvo, E. R. *Org. Lett.* **2008**, *11*, 485−488.

(59) Vitagliano, A.; Åkermark, B.; Hansson, S. *Organometallics* **1991**, *10*, 2592−2599.

(60) In contrast, oxidative addition of Pd(0) to allylic acetates and carbonates occurs reversibly to establish an equilibrium between the allylpalladium intermediate and the reactant. See: (a) Reference 55. (b) Amatore, C.; Gamez, S.; Jutand, A.; Meyer, G.; Moreno-Mañas, M.; Morral, L.; Pleixats, R. *Chem. Eur. J.* **2000**, *6*, 3372−3376.

(61) For the synthesis and stoichiometric reactions of an allylpalladium complex with a similar phosphinocarboxylate ligand, see: Knühl, G.; Sennhenn, P.; Helmchen, G. *J. Chem. Soc., Chem. Commun.* **1995**, 1845−1846.

(62) Kawatsura, M.; Ikeda, D.; Komatsu, Y.; Mitani, K.; Tanaka, T.; Uenishi, J. *Tetrahedron* **2007**, *63*, 8815−8824.

(63) (a) Kawatsura, M.; Ata, F.; Wada, S.; Hayase, S.; Uno, H.; Itoh, T. *Chem. Commun.* **2007**, 298−300. (b) Kawatsura, M.; Ata, F.; Hirakawa, T.; Hayase, S.; Itoh, T. *Tetrahedron Lett.* **2008**, *49*, 4873−4875. (c) Sundararaju, B.; Achard, M.; Demerseman, B.; Toupet, L.; Sharma, G. V. M; Bruneau, C. *Angew. Chem., Int. Ed.* **2010**, *49*, 2782−2785.

(64) (a) Yamamoto, T.; Saito, O.; Yamamoto, A. *J. Am. Chem. Soc.* **1981**, *103*, 5600−5602. (b) Tsuji, Y.; Kusui, T.; Kojima, T.; Sugiura, Y.; Yamada, N.; Tanaka, S.; Ebihara, M.; Kawamura, T. *Organometallics* **1998**, *17*, 4835−4841. (c) Chang, C.-W.; Norsikian, S.; Guillot, R.; Beau, J.-M. *Eur. J. Org. Chem.* **2010**, *2010*, 2280−2294.

(65) Like AgF, palladium complexes **5** and **8** are also sparingly soluble in benzene or toluene.

(66) (a) Breyer, D.; Braun, T.; Kläring, P. *Organometallics* **2012**, *31*, 1417−1424. (b) Martínez-Prieto, L. M.; Melero, C.; del Río, D.; Palma, P.; Cámpora, J.; Álvarez, E. *Organometallics* **2012**, *31*, 1425−1438.

(67) The reaction of **23** and **5** affords **24** within minutes, while hours are required for the production of **24** from AgF and **23**. The greater solubility of **5** may account for the rate difference.

(68) Although silver is known to adopt varying coordination modes, it is not clear how these coordination environments would affect the nucleophilicity of AgF. In contrast, we would expect the nucleophilicity of a palladium fluoride to vary in neutral and cationic intermediates.

(69) Cationic allylpalladium complexes of **L1** have been shown to equilibrate between a variety of coordination modes. See: Eastoe, J.; Fairlamb, I. J. S.; Fernández-Hernández, J. M.; Filali, E.; Jeffery, J. C.; Lloyd-Jones, G. C.; Martorell, A.; Meadowcroft, A.; Norrby, P.-O.; Riis-Johannessen, T.; Sale, D. A.; Tomlin, P. M. *Faraday Discuss.* **2010**, *145*, 27−47.

(70) (a) Amatore, C.; Jutand, A.; Meyer, G.; Mottier, L. *Chem. Eur. J.* **1999**, *5*, 466−473. (b) Amatore, C.; Gamez, S.; Jutand, A. *Chem. Eur. J.* **2001**, *7*, 1273−1280.

(71) Calculations indicate that halide exchange is exergonic by 3 kJ/mol. See Figure S10 (Supporting Information).

(72) Calculated C−F bond lengths in the product-coordinated Pd(0) complexes are 1.45−1.50 Å.

(73) The dihedral angle between the allyl or olefin plane and the Pd−P plane is a quantitative measure of the position of the transition state relative to the reactant or product. These values are presented in Table S3 (Supporting Information). Also see: Oslob, J. D.; Åkermark, B.; Helquist, P.; Norrby, P.-O. *Organometallics* **1997**, *16*, 3015−3021.

(74) In other Pd-catalyzed allylic alkylations, enantioselectivities of reactions with late transition states have been rationalized by calculating relative product energies: (a) Svensson, M.; Bremberg, U.; Hallman, K.; Csöregh, I.; Moberg, C. *Organometallics* **1999**, *18*, 4900−4907. (b) Hallman, K.; Frölander, A.; Wondimagegn, T.; Svensson, M.; Moberg, C. *Proc. Natl. Acad. Sci. U.S.A.* **2004**, *101*, 5400−5404.

(75) Kleimark, J.; Johansson, C.; Olsson, S.; Håkansson, M.; Hansson, S.; Åkermark, B.; Norrby, P.-O. *Organometallics* **2011**, *30*, 230−238.

(76) Pd(0)-catalyzed reactions of the acetate and carbonate analogues of **21** afford <5% yields of the allylic fluoride products when **5** is used as a fluoride source.

(77) (a) Becke, A. D. *J. Chem. Phys.* **1993**, *98*, 5648−5652. (b) Becke, A. D. *J. Chem. Phys.* **1993**, *98*, 1372−1377. (c) Lee, C.; Yang, W.; Parr, R. G. *Phys. Rev. B* **1988**, *37*, 785−789.

(78) Goodman, J. M.; Silva, M. A. *Tetrahedron Lett.* **2003**, *44*, 8233−8236.

(79) Kruse, H.; Goerigk, L.; Grimme, S. *J. Org. Chem.* **2012**, *77*, 10824−10834.

(80) Zhao, Y.; Truhlar, D. G. *Acc. Chem. Res.* **2008**, *41*, 157−167.

(81) Pangborn, A. B.; Giardello, M. A.; Grubbs, R. H.; Rosen, R. K.; Timmers, F. J. *Organometallics* **1996**, *15*, 1518−1520.

(82) Herrmann, W. A.; Broßmer, C.; Priermeier, T.; Öfele, K. *J. Organomet. Chem.* **1994**, *481*, 97−108.

(83) Boukerb, A.; Grée, D.; Laabassi, M.; Grée, R. *J. Fluorine Chem.* **1998**, *88*, 23−27.

(84) Umemoto, T.; Singh, R. P.; Xu, Y.; Saito, N. *J. Am. Chem. Soc.* **2010**, *132*, 18199−18205.